Bollettino di Geofisica Teorica ed Applicata Vol. 60, n. 3, pp. 419-432; September 2019
DOI 10.4430/bgta0264

Structural interpretation and reservoir characterisation of the Missa Keswal area, upper Indus basin, Pakistan

M. Abid[1,2], M. Riaz[3,4], M. Shah[5], T. Zafar[4,6] and A. Malik[7]

[1] *School of Ocean and Earth Science, Tongji University, Shanghai, China*
[2] *Department of Earth and Environmental Sciences, Bahria University, Islamabad, Pakistan*
[3] *School of Earth Sciences and Resources, China University of Geosciences, Beijing, China*
[4] *Institute of Geology, University of the Punjab, Lahore, Pakistan*
[5] *Women University Swabi, Swabi, Pakistan*
[6] *Institute of Geochemistry, Chinese Academy of Sciences, Guiyang, China*
[7] *LMK Resources Jinnah Avenue, Islamabad, Pakistan*

(Received: 24 August 2018; accepted: 10 December 2018)

ABSTRACT Accurately delineating the subsurface structures, lithologies and pore fluids is a prevalent procedure in reservoir characterisation. Subsurface structures are deciphered on the basis of seismic reflection data. However, seismic data on its own is inadequate to accurately mark fluid heterogeneities of pores buried in the subsurface. In this research, the integrated strategy of seismic interpretation, rock physics modelling and fluid substitution scrutiny has been conducted to exemplify the reservoir potential of the Missa Keswal area of Pakistan. Seismic data interpretation revealed that Eocene limestone is a prospective reservoir in the study area. Structural interpretation reveals a compressional regime with the presence of a pop-up structure restricted by thrusts on either sides, which is appropriate for hydrocarbon accumulation. In addition, instantaneous amplitude affirms the recognition of foremost lithological changes and discontinuities. Anomalous regions were identified by bulk modulus and Poisson ratio which are indicators of valuable rock physics parameters. Gassmann fluid substitution performed at Eocene level implies discrepancy in acoustic properties at diverse levels of water saturation. The presented integration approach can be applied to assess reservoir potential in any sedimentary basin of the world with available conventional data.

Key words: 2D seismic interpretation, attribute analysis, rock physics, Gassmann fluid substitution, Missa Keswal.

1. Introduction

The main task of seismic interpretation is to characterise subsurface geological structures and lithologies with high levels of precision. Analysis of seismic data allows to distinguish hydrocarbon from non-hydrocarbon-bearing rocks (Al-Sadi, 1980; Badley, 1985; Lines and Newrick, 2004). Conversely, it is tricky to distinguish a payable hydrocarbon interval from a non-payable interval through the interpretation of seismic data only (Khalid and Ghazi, 2013). There are numerous reports which used only 2D seismic data for retrieving the consequences;

however, reliability of the results was scarce and led towards drilling of dry holes (Khalid and Ghazi, 2013). To substitute these problems, quantitative seismic analysis techniques have been introduced in the field of reservoir characterisation. According to Khalid *et al.* (2015), several tactics, specifically seismic attributes, rock physics modelling and fluid saturation, are extensively used in the procedures of seismic portrayal. Increase of water saturation is the main reason for failure of a development well. Obtained water saturation information through seismic data is reasonably complex, unless we incorporate rock physics modelling (Avseth *et al.,* 2005). Fluid substitution on well data provides a tool for fluid identification and quantification in a reservoir (Krief *et al.,* 1990; Russell *et al.,* 2003; Han and Batzle, 2004; Kumar, 2006; Nguyen and Myung, 2011).

Potwar sub-basin in Pakistan (Fig. 1) is the oldest reservoir, immensely rich in oil and gas (Kadri, 1995; Ghazi *et al.,* 2014; Khalid *et al.,* 2015). Several researchers (Moghal *et al.,* 2007; Hasany and Saleem, 2012; Ghazi *et al.,* 2014; Riaz *et al.,* 2018, 2019) described the hydrocarbon potential of Potwar basin on the basis of seismic depiction. However, quantitative presentation of seismic amplitude anomalies related to the pore fluid variations was ignored. The prime objective

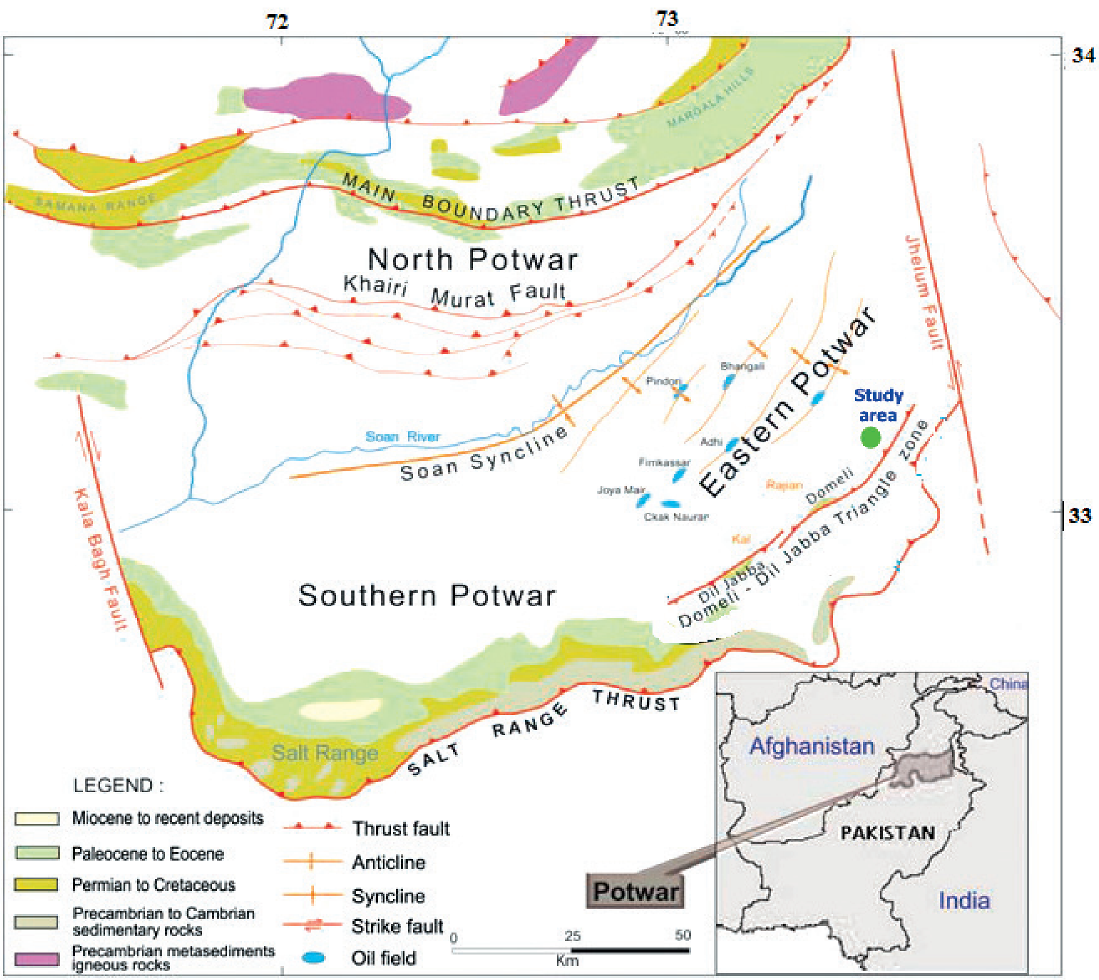

Fig. 1 - Location and structural boundaries of the study area (modified after Aamir and Siddiqui, 2006; Riaz *et al.,* 2018, 2019).

of this research work is to apply quantitative seismic techniques for reservoir characterisation and field development of the Missa Keswal area in the Potwar sub-basin of Pakistan.

2. Geological setting

The Missa Keswal area (32° 12’ to 32° 55’ N; 72° 22’ to 72° 55’ E) lies in the Potwar sub-basin, which is part of the upper Indus basin, Pakistan (Fig. 1). Structurally, the Potwar sub-basin is bounded to the north by the Main Boundary Thrust (MBT), to the south by the Salt Range Thrust (SRT), to the east by the Jhelum fault and to the west by the Kalabagh fault (Kazmi and Rana, 1982; Aamir and Siddiqui, 2006). The study area shows a compressional regime with the presence of pop-up structures along with thrusts and tight anticlines that represent the prevailing features of the Potwar area (Moghal *et al.,* 2007; Riaz *et al.,* 2018, 2019). The E-W Soan syncline (Fig. 1) divides the area (Jadoon *et al.,* 2003; Shahzad *et al.,* 2009; Mehmood *et al.,* 2016; Riaz *et al.,* 2018) into the more deformed northern Potwar Deformed Zone (NPDZ) and the less deformed southern Potwar Platform Zone (SPPZ).

Stratigraphically, the Potwar sub-basin (Fig. 2) contains sediments deposited during the Precambrian to Quaternary age (Kazmi and Jan, 1997). These authors suggested that the Potwar sub-basin is filled with sediments of Cambrian evaporites, which are overlain by the deposits of Cambrian to Eocene age. Furthermore, thick Miocene and Pliocene molasses overlie these deposits. The buckling of this entire section is due to the Himalayan orogeny during the Pliocene to middle Pleistocene (Moghal *et al.,* 2007). Diverse unconformities are accountable for interrupting the whole depositional sequence of Potwar sub-basin. The most noteworthy unconformity is between Cambrian and Permian as well as between the Eocene and Miocene (Khan *et al.,* 1986).

3. Available data resource

The data used in the present work consist of 12 2D seismic reflection lines and a common suite of logs comprising caliper, Gamma ray (GR), sonic, density, and resistivity of Missa Keswal-01 and Missa Keswal-02 wells and interpreted formation tops (Fig. 3). Out of 12 seismic lines, seven lines are in the direction of dip (NW-SE) and five lines are acquired in strike direction (NE-SW). The data was attained from the Directorate General Petroleum Concession, Government of Pakistan.

4. Methodology

In this study, the adopted methodology was accomplished into two key parts; the first is to interpret and perform attribute analysis on available 2D seismic data. The second part is to calculate rock physics parameters and fluid substitution analysis: Fig. 4 portrays the workflow trailed in this study to conduct constructive information from the available data.

2D seismic data was initially interpreted to identify the structural trend by observing the lateral discontinuity of the horizon induced by the presence of faults. Based on continuity and sharp

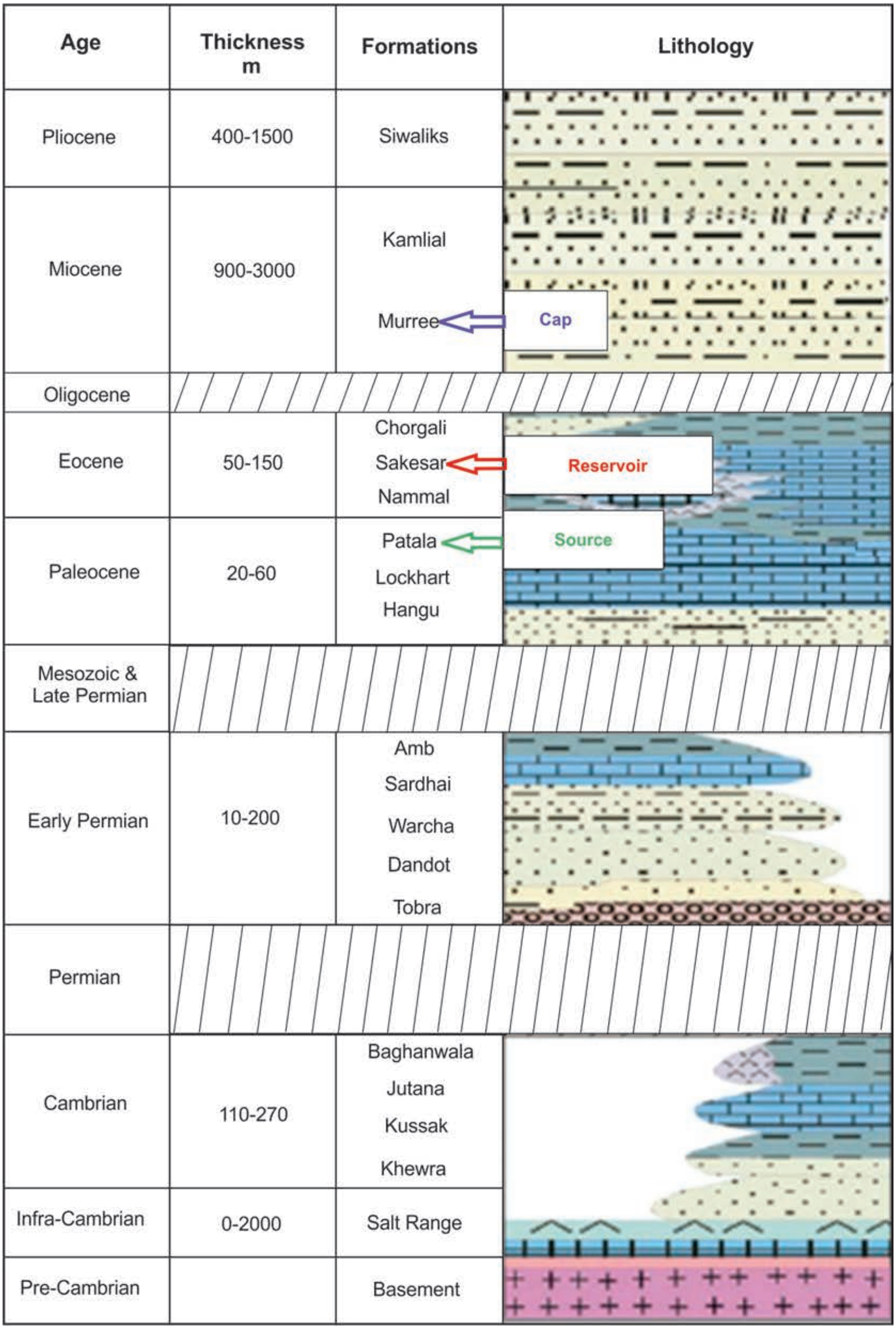

Fig. 2 - Stratigraphic column of eastern Potwar sub-basin (modified after Aamir and Siddiqui, 2006).

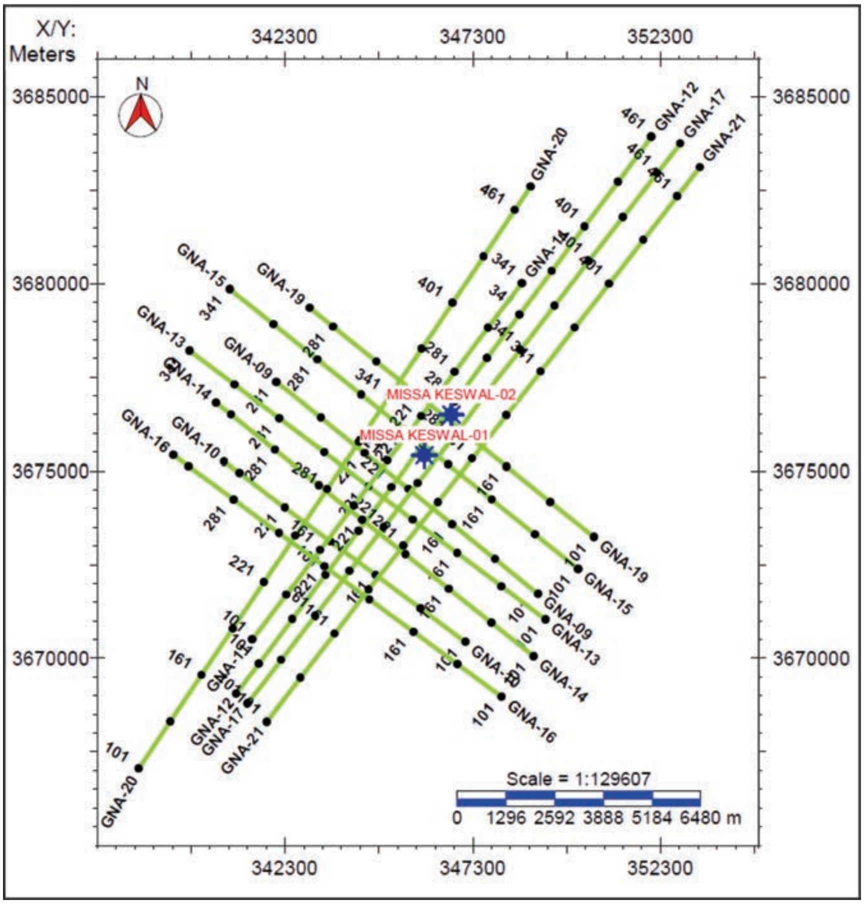

Fig. 3 - Base map with orientation of seismic lines and wells.

acoustic impedance contrast, two horizons (top of the Eocene package and top basement) were identified along the whole area. Two-way travel time structure map on top of Eocene package was mapped.

In structural interpretation, velocity is the most important parameter that is used for time to depth conversion. In this paper, the velocity analysis was performed after generating the time maps. Vertical velocity at the locations of wells was already available through a sonic log; for lateral control of velocity, a dummy check-shot was generated. Time and RMS velocity values were noted from the velocity panels mentioned on the top of each seismic line (DIP line). These RMS velocities were converted to interval and average velocities through Dix (1955) equation at millisecond time intervals.

Moreover, noting down the time of the particular horizons from the digitally interpreted sections, against that time average velocity values were perceived. In addition, the same procedure was implemented on all the seismic dip lines. After performing this methodology, a number of velocity control points along the entire study area were achieved (Fig. 5). Lastly, by using all these velocities, a final map was prepared.

By using these velocities, depth conversion was carried out and depth maps at the level of marked horizons were generated.

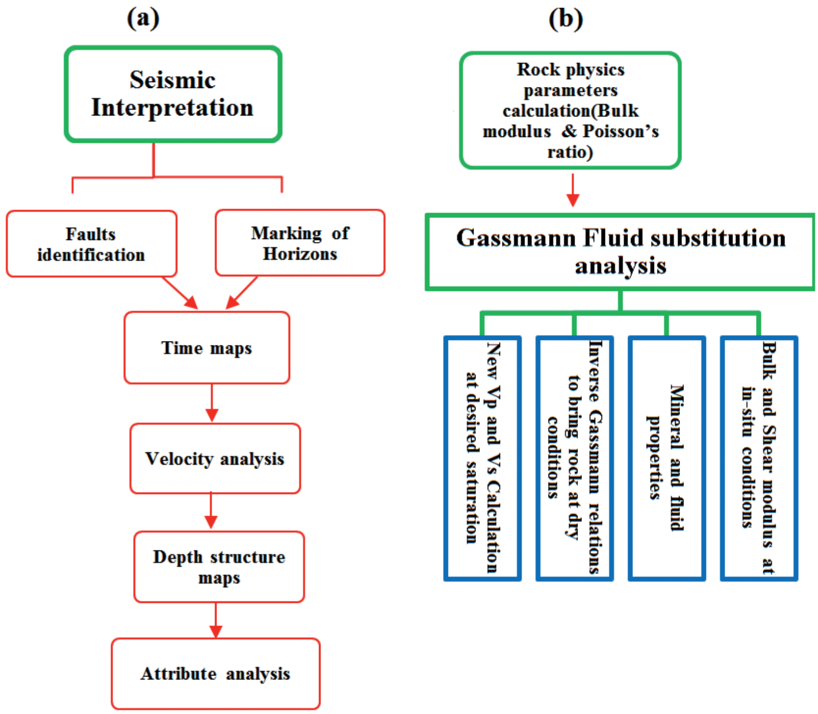

Fig. 4 - Workflow: a) seismic interpretation; b) Gassmann fluid substitution.

After seismic interpretation, attribute analysis was performed on the available data in bi-dimension. The most appropriate attribute that provides us results is the instantaneous amplitude attribute. Instantaneous amplitude is the square root of the total energy of the seismic signal at any instant of time. It is the envelope of the seismic trace (Taner *et al.*, 1979). For each time sample, reflection strength is calculated as follows:

$$Reflection\ Strength = \sqrt{(recorded\ trace)^2 + (quadrature)^2} \tag{1}$$

Two rock physics parameters (bulk modulus and Poisson's ratio) were calculated at the top Eocene marked horizon. P-wave velocity was obtained from a sonic log and its conversion to S-wave was done using the equation by Castagna *et al*. (1985).

Bulk modulus (K) was calculated by:

$$K = \rho\left(Vp^2 - \frac{4}{3}Vs^2\right) \tag{2}$$

where, K is bulk modulus, ρ is the density, V_p and V_s are P- and S-wave velocities.

Poisson's ratio (σ) is the ratio of compressibility and rigidity. It was calculated using the following equation:

$$\sigma = \frac{0.5(VP^2 - 2Vs^2)}{(Vp^2 - Vs^2)} \tag{3}$$

where V_p and V_s represent P-wave velocity and S-wave velocity, respectively.

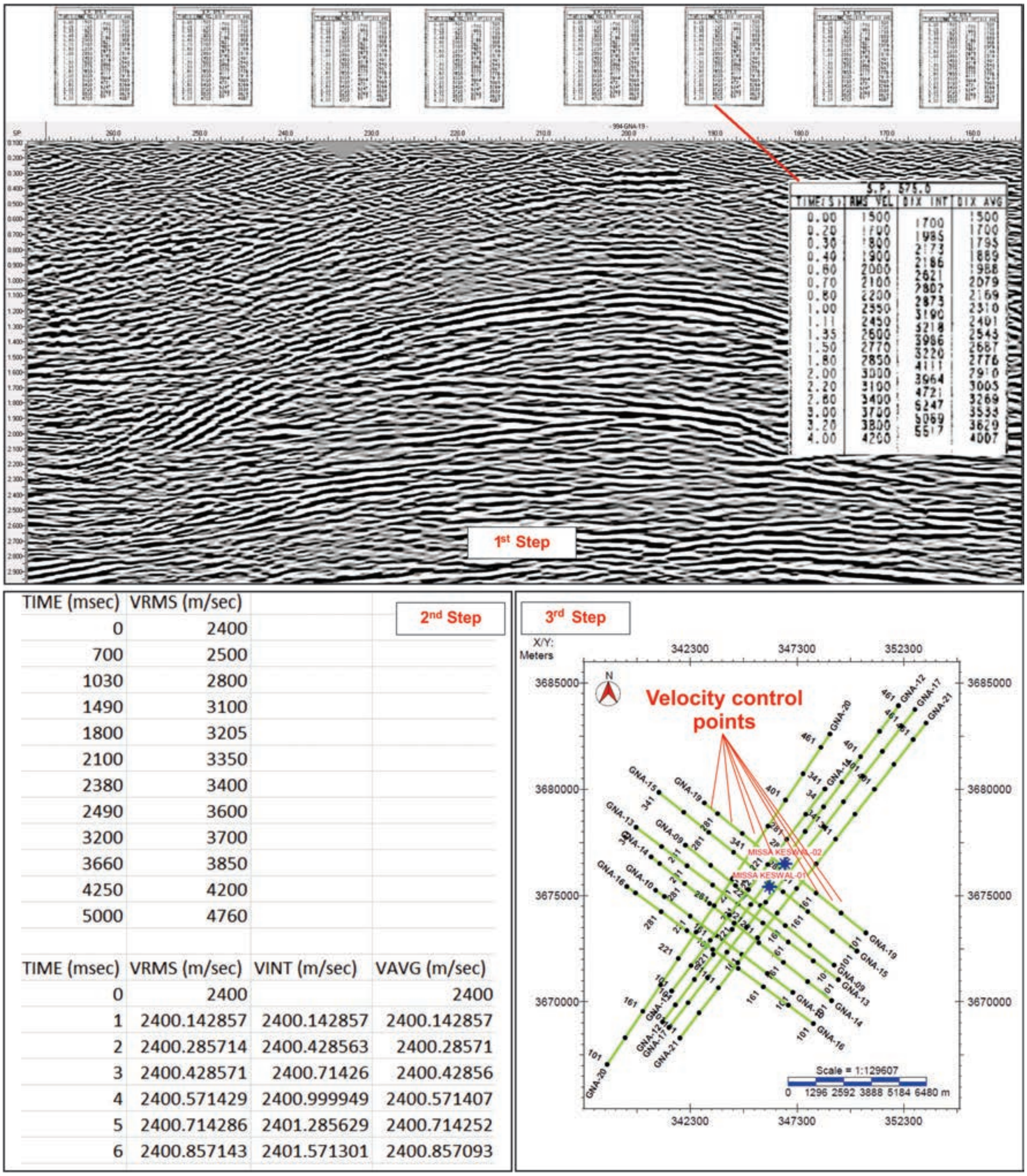

TIME (msec)	VRMS (m/sec)
0	2400
700	2500
1030	2800
1490	3100
1800	3205
2100	3350
2380	3400
2490	3600
3200	3700
3660	3850
4250	4200
5000	4760

TIME (msec)	VRMS (m/sec)	VINT (m/sec)	VAVG (m/sec)
0	2400		2400
1	2400.142857	2400.142857	2400.142857
2	2400.285714	2400.428563	2400.28571
3	2400.428571	2400.71426	2400.42856
4	2400.571429	2400.999949	2400.571407
5	2400.714286	2401.285629	2400.714252
6	2400.857143	2401.571301	2400.857093

Fig. 5 - Velocity modelling methodology.

Finally, fluid substitution analysis was performed in desired zone to delineate the structure. In recent times, relating dry and saturated rocks velocities has become a critical part of rock physics (Avseth *et al.,* 2005; Mavko *et al.,* 2009). P-wave velocity (V_p), S-wave velocity (V_s) and density are key parameters that control the seismic response of reservoir. Discrepancy in the above-mentioned seismic properties can be predicted by fluid substitution analysis. The initial step of fluid substitution was to calculate saturated bulk modulus (K_{sat}), obtained by applying Eq. 2 as describe above for *in-situ* conditions.

The second step was to bring rock at dry conditions in order to calculate the dry bulk modulus (K_{dry}), for that purpose the equation given by Zhu and McMechan (1990) was used:

$$K_{dry} = \frac{k_{sat}\left(\frac{\phi Kmat}{Kfl} + 1 - \phi\right) - Kmat}{\frac{\phi Kmat}{Kfl} + \frac{Ksat}{Kmat} - 1 - \phi} \tag{4}$$

where K_{sat}, K_{mat}, and K_{fl} represent the bulk moduli of saturated rock, of the matrix, and the fluid, respectively, whereas ϕ is the porosity. The porosity was evaluated from well logs interpretation. The mineral matrix recognition was obtained from logging results.

Matrix bulk modulus was calculated by using the Voigt-Ruess-Hill averaging method (Hill, 1952):

$$K_{mat} = \frac{1}{2}\left[(V_{clay}K_{clay} + V_{calcite}K_{calcite}) + \left(\frac{V_{clay}}{K_{clay}} + \frac{V_{calcite}}{K_{calcite}}\right)\right] \tag{5}$$

where V_{clay} and $V_{calcite}$ are the volume of clay (shale) and calcite (limestone) within the matrix, K_{clay} and $K_{calcite}$ are the relative bulk moduli. The clay volume was estimated by Gamma ray log (Asquith *et al.,* 2004), and calcite volume attained by subtracting clay volume from total volume of rock. The bulk modulus (K) for clay and calcite was obtained from Mavko *et al*. (2009). Mineral matrix density was estimated by averaging the densities of individual minerals (Kumar, 2006):

$$\rho_{mat} = V_{clay}\rho_{clay} + V_{clacite}\rho_{calcite} \tag{6}$$

where ρ_{clay} and $\rho_{calcite}$ are calcite and clay densities, respectively. For fluid mixture determination, Wood's relations were used (Wood, 1955). Mixtures of fluids are analysed following this method:

$$\frac{1}{K_{fl}} = \frac{S_w}{K_{brine}} + \frac{S_{Hc}}{K_{hyc}} \tag{7}$$

$$\rho_{fl} = S_{w\rho brine} + SH_{\rho hyc} \tag{8}$$

where S_w is the saturation of water obtained from resistivity log (Asquith *et al.,* 2004), SH=(1−S_w) is the saturation of hydrocarbon. K_{brine} and K_{hyc} are bulk moduli of water and hydrocarbons (oil or gas), whereas ρ_{hyc} and ρ_{brine} are the densities of hydrocarbons and water. All of these parameters, including K_{brine}, K_{hyc}, ρ_{brine}, and ρ_{hyc} were calculated by initial well conditions at reservoir level using Batzle and Wang (1992) relations.

Once bulk modulus of dry rock was determined, we used it for the calculation of saturated bulk modulus of a rock at the desired saturation by using original Gassmann (1951) relations:

$$k_{sat} = k_{dry} + \frac{\left(1 - \frac{k_{dry}}{k_{mat}}\right)^2}{\left[\frac{\phi}{k_{fl}} + \frac{(1-\phi)}{k_{mat}} - \frac{k_{dry}}{k^2_{mat}}\right]} \tag{9}$$

and

$$\mu_{sat} = \mu_{dry} \tag{10}$$

where, in the above equations μ_{sat} and μ_{dry} are saturated and dry shear moduli. From Eq. 10, it is clear that shear modulus is independent of fluid presence. There is no effect of changing saturation on shear modulus of the rock sample. The density at desired saturation was calculated by the following equation (Kumar, 2006):

$$\rho_{sat} = \phi \rho_{fl} + (1-\phi)\rho_{mat} \tag{11}$$

For the calculation of (saturated) V_p and V_s after fluid substitution, the following equations were used (Kumar, 2006):

$$Vp = \sqrt{\frac{k + 4/3\mu}{\rho}} \tag{12}$$

and

$$Vs = \sqrt{\mu / \rho}\ . \tag{13}$$

5. Results

5.1. Seismic interpretation

In the first part of the seismic portrayal, two horizons, i.e. top Eocene package and top basement, were discernible on the basis of character and continuity. Two major thrusts F1 and F2 bound the pop-up anticlinal structure (Fig. 6). The green colour indicates the top Eocene package and yellow represents the top basement, whereas F1 and F3 in blue colour are depiction of major thrusts. Seismic interpretation results reveal the presence of a pop-up anticlinal structure bounded by thrusts on either sides in the study area where the orientation of the major faults is NW-SE.

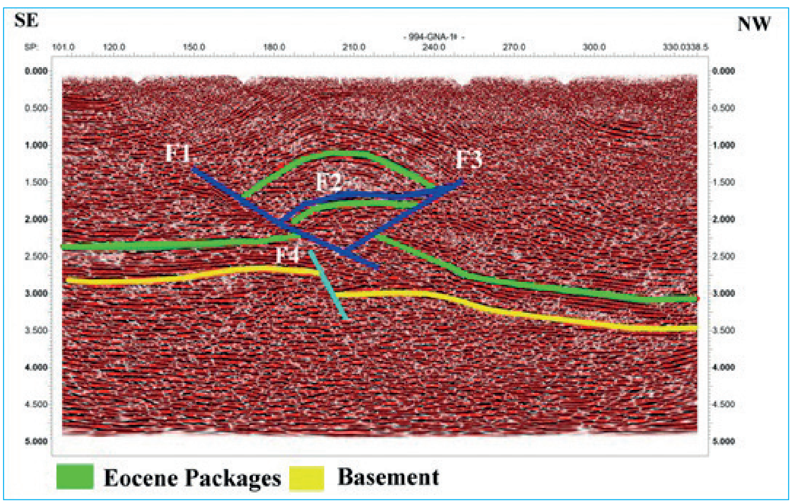

Fig. 6 - Interpreted time section of seismic line 994-GNA-19 showing major horizons and faults.

Two-way time structure map of top Eocene package is revealed in Fig. 7a. From time map it is obvious that the study area is enclosed by two major thrust faults. The time contour range is 1250 ms to 3000 ms. The high areas exhibit shallow level with low time values on the map. The low areas indicate a deeper level and higher time values. From time section, the locations of the wells can be perceived. Red colour denotes low time values while blue represents high time values. The contours of the two-way travel time are closed on the up thrown block representing a thrust anticline.

From velocity analysis, velocity contour maps have been prepared. The red colour depicts the lowest velocity values and the blue colour shows the highest velocity ones (Fig. 7b). This particular map indicates velocity variation across the study area. Time maps were converted into depth maps by using the velocity obtained from the velocity analysis. In depth map, orientation and the dip of the structure are similar to the related time structure map. Fig. 7c shows that the depth range is from 1498 m to 5542 m.

5.2. Attribute analysis

Instantaneous amplitude section is presented in Fig. 8. The amplitude variations observed in the instantaneous amplitude map range from 3 to 10, where the dark blue shading depicts high

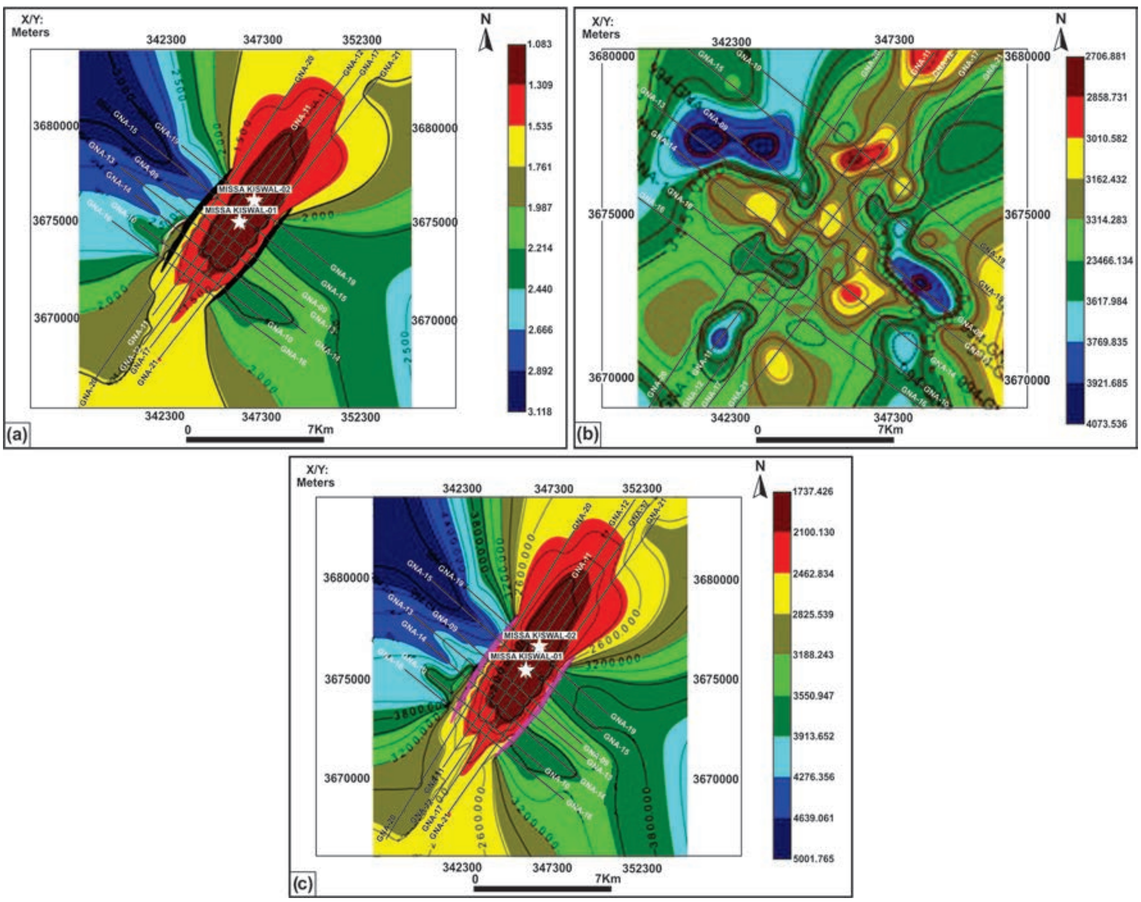

Fig. 7 - a) Two-way time contour map at the level of Eocene package showing favourable leads for hydrocarbons accumulation; b) velocity contour map depicting velocity variations in the study area; c) depth contour map at the level of Eocene package.

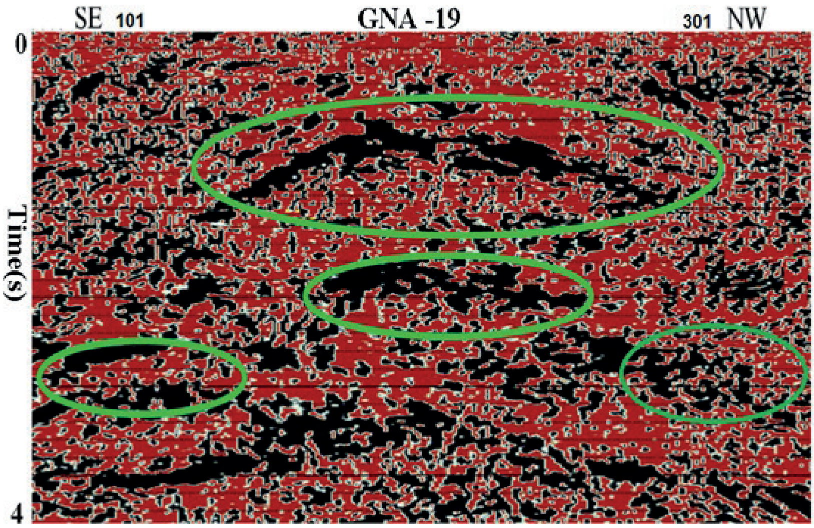

Fig. 8 - Instantaneous amplitude section showing discontinuities and reflectors (highlighted with green ellipses).

amplitude and red shading indicates low amplitude. Reflectors and faults are clearly visible as a confirmation of the interpretation results.

5.3. Rock physics parameters

The calculated bulk modulus on our acquired data is in the range of 11.63-24.63 GPa (Fig. 9a). Low values of bulk modulus indicate the presence of hydrocarbons, confirmed by the measurements at drill location.

Poisson's ratio for the Eocene unit is calculated on all the seismic lines and, then, contoured in accordance with the original lines (Fig. 9b). The values of Poisson's ratio are in the range of 0.25 and 0.38. The low Poisson's ratio values reveal depletion in the portion comprised of hydrocarbon. An anomalous zone has a high Poisson's ratio which is confirmed by well location.

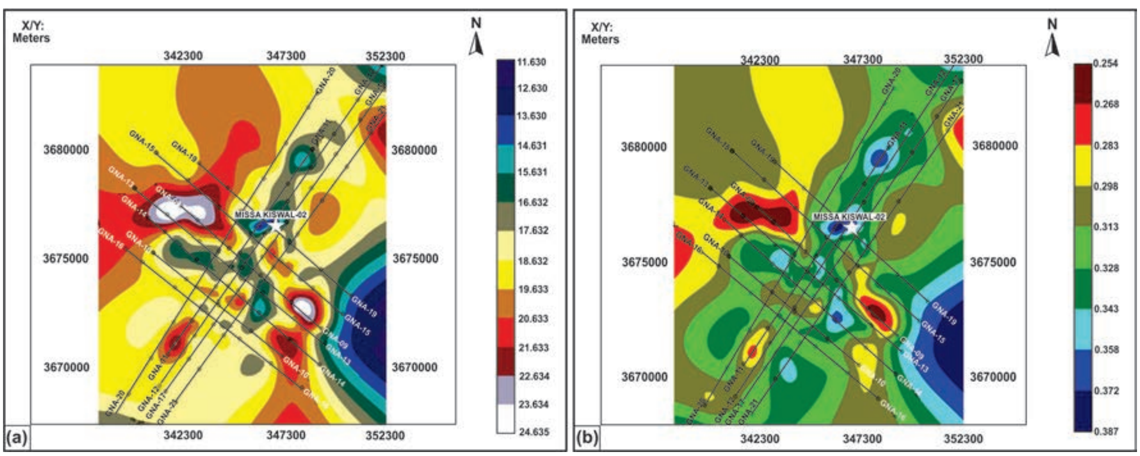

Fig. 9 - Bulk modulus (a) and Poisson's ratio (b) maps, depicting the anomalous zone with comparatively low bulk modulus and high Poisson's ratio values.

5.4. Fluid substitution

In this section the results of Gassmann fluid substitution are discussed in the context of hydrocarbon monitoring (Fig. 10a). Results represent the variation in P-wave velocity at 80% and 100% saturation of water as compared to the original saturation. From the results, it can also be observed that the P-wave velocity values increase quite significantly when the saturation of water increases. By contrast, the maximum V_p was found at 100% saturation. There is no increase in S-wave velocity because shear modulus is not dependent on fluid type (Eq. 10). The results indicate an almost comparable trend in all saturations, very small differences can be seen in Fig. 10b. This slight change was due to a change in density.

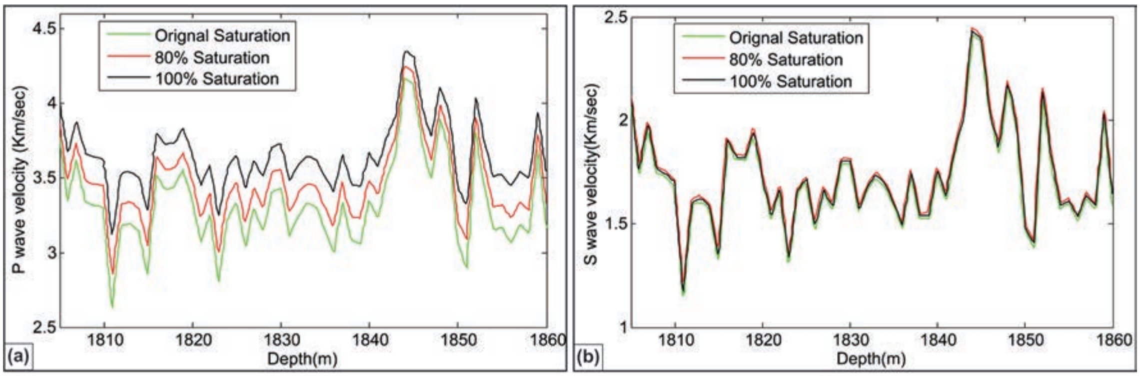

Fig. 10 - Variations in: a) P-wave velocity; b) S-wave velocity, at original, 80%, and 100% water saturation levels.

6. Discussion

Reservoir characterisation is a process to illustrate diverse reservoir properties by using all the available data. In this research, the reservoir depiction techniques were implemented on the data of the Missa Keswal area in the upper Indus basin in Pakistan. The identified faults indicate that the area lies in the compressional regime. The structure is primarily restricted by thrusts on either side (Fig. 6). The time structure map (Fig. 7a) on the top of the Eocene unit shows the time variations from 1.083 s to 3.118 s. On time map, the blue colour represents the deepest part of the horizon while the red colour shows the lowest part. Both wells Missa Keswal-01 and 02 are drilled on top of the structural high. The same trend is followed in the depth contour map. In addition, instantaneous amplitude of seismic data highlights the major lithological changes and discontinuities (Fig. 8). Different rock physics parameters calculated in this study help us to distinguish the reservoir and non-reservoir zone.

In the final part of this research, fluid substitution application was performed on the area to prevent the failure in the planning of the development well, which will be drilled in the proposed sites in future. The reservoir seismic properties (velocity and density) vary when hydrocarbon is extracted. In other words, the impact on seismic properties due to hydrocarbon depletion can be observed. Moreover, fluid substitution provides us a means to predict the seismic response for dissimilar saturation levels. In fact, the original water and hydrocarbon saturation from a petrophysical analysis of the available logging data, was calculated at 35% and 65%, respectively. The models of 80% water saturation means 20% will be hydrocarbon. Finally, models of 100%

mean the reservoir will be fully saturated with water (Figs. 10a and 10b). Furthermore, there is a slight change in S-velocity at both saturation levels, which is owing to density change, as shear modulus is independent of fluid presence.

Variation of the acoustic impedance contrast for all saturation models, is due to changes in P-wave velocity and density. These variations in acoustic impedance can be used to organise a synthetic seismogram for each saturation model. We can simulate it with innovative acquired and evaluated seismic data at the well location, as structure and subsurface architecture will not change. Consequently, in this research at different levels of water saturation, acoustic properties were compared with the initial model at *in-situ* conditions of the well.

7. Conclusions

In this study, seismic and attribute interpretation, rock physics calculations, and Gassmann fluid substitution analysis, were applied to characterise the reservoir potential of Missa Keswal (upper Indus basin, Pakistan). Seismic interpretation reveals that the pop-up structure is bounded by thrusts on either sides and is a suitable trap for hydrocarbon accumulation. Furthermore, this trap is also confirmed by time and depth contour maps. Instantaneous amplitude has proven to be of great importance in detecting major lithological changes and also has the potential to delineate the location of the main discontinuities.

Bulk modulus and Poisson's ratio are useful rock physics parameters to identify anomalous regions in the study area. Hydrocarbon zones have high Poisson's ratio and low bulk modulus values. Gassmann fluid substitution performed at Eocene level indicates the variation in elastic properties at different levels of water saturation. The modelled response was performed at original, 80% and 100% water saturation level. These variations in elastic properties can be utilised in forward modelling to generate a synthetic seismogram, and comparing with newly acquired seismic data (if available), will reduce the risk of well failure during the developmental phase.

Acknowledgements. We would like to acknowledge the Chinese government for providing indoor facilities for this research. We are also thankful to the Department of Earth and Environmental Sciences Bahria University that allowed us to use their workstation facility.

REFERENCES

Aamir M. and Siddiqui M.M.; 2006: *Interpretation and visualization of thrust sheets in a triangle zone in eastern Potwar, Pakistan*. The Leading Edge, **25,** 24-37.

Al-Sadi H.N.; 1980: *Seismic exploration technique and processing*. Birkhauser Verlag, Basel, Switzerland, 215 pp.

Asquith G.B., Krygowski D. and Gibson C.R.; 2004: *Basic well log analysis: methods in exploration, Vol. 16*, *2nd ed*. Am. Ass. Pet. Geol., Tulsa, OK, USA, 244 pp.

Avseth P., Mukerji T. and Mavko G.; 2005: *Quantitative seismic interpretation. Applying rock physics tools to reduce interpretation risk*. Cambridge University Press, Cambridge, UK, 374 pp.

Badley M.; 1985: *Practical seismic interpretation*. Int. Human Res. Dev. Corporation, Boston, MA, USA, 266 pp.

Batzle M. and Wang Z.; 1992: *Seismic properties of pore fluids*. Geophys., **57,** 1396-1408.

Castagna J.P., Batzle M.L. and Eastwood R.L.; 1985: *Relationships between compressional-wave and shear-wave velocities in clastic silicate rocks*. Geophys., **50,** 571-581.

Dix C.H.; 1955: *Seismic velocities from surface measurements*. Geophys., **20,** 68-86.

Gassmann F.; 1951: *Uber die elastizitat poroser Medien*. Vierteljahrsschr. Naturforsch. Ges. Zürich, **96,** 1-23, in German.

Ghazi S., Aziz T., Khalid P. and Sahraeyan M.; 2014: *Petroleum play analysis of the Jurassic sequence, Meyal-field, Potwar basin, Pakistan*. J. Geol. Soc. India, **84,** 727-738.

Han D.H. and Batzle M.L.; 2004: *Gassmann's equation and fluid-saturation effects on seismic velocities*. Geophys., **69,** 398-405.

Hasany S.T. and Saleem U.; 2012: *An integrated subsurface geological and engineering study of Meyal field, Potwar plateau, Pakistan*. Search and Discovery, Art. 20151.

Hill R.; 1952: *The elastic behavior of a crystalline aggregate*. Proc. Phys. Soc., section A, **65,** 349-354.

Jadoon I.A.K., Shami B.A. and Abbasi I.A.; 2003: *Fracture analysis of Khaur anticline and its implications on subsurface fracture system*. PAPG-SPE Annual Technical Conference and Oil Show, Islamabad, Pakistan, pp. 235-250.

Kadri I.; 1995: *Petroleum geology of Pakistan*. Pakistan Petroleum Limited, Karachi, Pakistan, 275 pp.

Kazmi A. and Rana R.; 1982: *Tectonic map of Pakistan*. Geol. Surv. Pakistan, **39,** 283-300.

Kazmi A.H. and Jan M.; 1997: *Geology and tectonics of Pakistan*. Graphic Publishers, Karachi, Pakistan, 528 pp.

Khalid P. and Ghazi S.; 2013: *Discrimination of fizz water and gas reservoir by AVO analysis: a modified approach*. Acta Geod. Geophys., **48,** 347-361.

Khalid P., Yasin Q., Sohail G. and Kashif J.M.; 2015: *Integrating core and wireline log data to evaluate porosity of Jurassic formations of Injra-1 and Nuryal-2 wells, western Potwar, Pakistan*. J. Geol. Soc. India, **86,** 553-562.

Khan M., Ahmed R., Raza H.A. and Kemal A.; 1986: *Geology of petroleum in Kohat-Potwar depression, Pakistan*. Am. Assoc. Pet. Geol. Bull., **70,** 396-414.

Krief M., Garat J., Stellingwerff J. and Ventre J.; 1990: *A petrophysical interpretation using the velocities of P and S waves (Full-waveform sonic)*. Log Analyst, **31,** 355-369.

Kumar D.; 2006: *A tutorial on Gassmann fluid substitution: formulation, algorithm and Matlab code*. Geohorizons, **11**, 4-12.

Lines L.R. and Newrick R.T.; 2004: *Fundamentals of geophysical interpretation*. Soc. Explor. Geophys., Geophys. monograph series n. 13, 274 pp.

Mavko G., Mukerji T. and Dvorkin J.; 2009: *The rock physics handbook: tools for seismic analysis of porous media, 2nd ed*. Cambridge University Press, Cambridge, UK, 339 pp., doi: 10.1017/CBO9780511626753.

Mehmood W., Aadil N. and Jadoon Y.K.; 2016: *3-D Structural modeling of Meyal Field, Potwar sub-basin, Pakistan using seismic and well data*. The Nucleus, **53,** 26-32.

Moghal M.A., Hameed A., Saqi M.I. and Bugti M.N.; 2007: *Subsurface geometry of Potwar sub-basin in relation to structuration and entrapment*. Pakistan J. Hydrocarbon Res., **17,** 61-72.

Nguyen P.T. and Myung J.N.; 2011: *A review on methods for constructing rock physics model of saturated reservoir rock for time-lapse seismic*. Geosyst. Eng., **14,** 95-107.

Riaz M., Pimentel N., Ghazi S., Zafar T., Alam A. and Ariser S.; 2018: *Lithostratigraphic analysis of the Eocene reservoir units of Meyal Area, Potwar Basin, Pakistan*. Himal. Geol., **39**, 72-81.

Riaz M., Pimentel N., Ghazi S., Zafar T. and Jafarian A.; 2019: *2D seismic interpretation of Meyal Area, northern Potwar Deform Zone (NPDZ), Potwar Basin, Pakistan*. Open Geosci., **11**, 1-16.

Russell B.H., Hedlin K., Hilterman F.J. and Lines L.R.; 2003: *Fluid property discrimination with AVO: a Biot-Gassmann perspective*. Geophys., **68,** 29-39.

Shahzad F., Mahmood S.A. and Gloaguen R.; 2009: *Drainage network and lineament analysis: an approach for Potwar Plateau (northern Pakistan)*. J. Mt. Sci, **6,** 14-24.

Taner M.T., Koehler F. and Sheriff R.; 1979: *Complex seismic trace analysis*. Geophys., **44,** 1041-1063.

Wood A.B.; 1955: *A textbook of sound: being an account of the physics of vibrations with special reference to recent theoretical and technical developments,* 3rd ed. The Macmillan Co., New York, NY, USA, 636 pp.

Zhu X. and McMechan G.A.; 1990: *Direct estimation of the bulk modulus of the frame in a fluid-saturated elastic medium by Biot Theory.* In: Expanded Abstracts, SEG Technical Program 1990, Society of Exploration Geophysicists, pp. 787-790, doi: 10.1190/1.1890340.

Corresponding author: Muhammad Riaz
School of Earth Sciences and Resources, China University of Geosciences,
Institute of Geology, University of the Punjab, Lahore, Pakistan.
Xueyuan Road, No. 29, Haidian District, Beijing, 100083 P.R. China
Phone: + 923339834262; e-mail: riazjass@yahoo.com